

Impact of machining strategy on OFE copper for SRF applications

BELKHIR F.^{1,2,a}, KOLENIC M.^{1,b*}, RECH J.^{2,c}, PÉREZ FONTENLA A.T.¹,
ROSAZ G.¹, MOROS A.¹, GARLASCHÈ M.¹, LEITH S.¹, NAISSON P.¹,
CARLOS C.P.A.¹

¹CERN, Geneva, Switzerland

²Centrale Lyon ENISE, Saint-Etienne, France

^a faudel.belkhir@cern.ch, ^b michal.kolenic@cern.ch, ^c joel.rech@enise.fr

Keywords: Surface Integrity, Machining, SRF, Cavity, OFE Copper, Niobium, SEM, FIB, GIXRD, FCC

Abstract. The study evaluates the impact of various milling strategies - on the surface and subsurface quality of an Oxygen-Free Electronic (OFE) copper substrate, and subsequently on the niobium (Nb) coating performance- for Superconducting Radio Frequency (SRF) cavities. Several cutting tools, cutting conditions and machining paths are compared, given their paramount influence in the final ‘SRF’ quality of the machined surfaces. The near surface region is evaluated by different means: surface roughness and shape accuracy are measured using a profilometer and Coordinate Measuring Machine (CMM) respectively; the thickness of the layer affected by machining on the OFE copper substrate is estimated by Focused Ion Beam Scanning Electron Microscopy (FIB - SEM). The dislocation density in the near surface layer is assessed by Grazing Incidence X-Ray Diffraction (GI-XRD) in both the OFE copper substrate and afterwards in the niobium coating. Main investigation results are discussed, and conclusions drawn for new guidelines on machining strategy and for future research developments.

Introduction

Radio Frequency Accelerating cavities are an essential part of particle colliders, as they provide energy to the charged particle beams for impact. As in many particle accelerators, SRF cavities are used in the Large Hadron Collider (LHC) at CERN; these are composed of an OFE copper (Cu) substrate, onto which a coating of superconducting niobium (Nb) is deposited via sputtering.

For optimizing the accelerating capability of SRF cavities, the surface integrity of the Niobium layer plays a key role [1]. It is known how machining OFE copper presents challenges due to its thermo-structural behaviour during cutting, its proneness to tool adhesion and to formation of build-up edges.

This study thus aims to explore the effects of various machining configurations on OFE copper substrates, to quantify and eventually to optimize their impact on substrate surface integrity, thus subsequently on the deposited Nb layer.

This study falls within a larger ongoing campaign at CERN: previous investigations focused on turning applications [2], revealing notable effects of cutting conditions on the subsurface layer of the copper substrate, particularly in terms of thickness and grain structure of the affected subsurface layers.

In the following, the campaign is extended to the examination of milling applications. The chosen case for this study is the Slotted Waveguide Elliptical (SWELL) cavity *Fig. 1*, a promising fully milled concept [3], under study for high energy applications such as the Future Circular Collider (FCC) of CERN [4]. The samples used in the study have first been machined, then surface treated, then tested and measured, as described in the following chapter.

Experimental Setup and Methodology

Fig. 1 shows two of the four Copper quadrants, of which the SWELL cavity is composed; the internal dark grey surface indicates the area undergoing subsequent Nb coating. The central bottom area of the cavity (Fig. 1) has been identified as area of interest, for obtaining the samples: when the cavity is powered, such area is subjected to the highest-intensity magnetic fields; while -in relation to fabrication via milling- the position and configuration of such area leads to low effective cutting speed - thus uncontrolled cutting [5]- during production of the given cavity. In order to reduce sample size and costs, discs (Ø84 x 10) containing only the area of interest have been produced, as shown in Fig. 2. Each milled profile (red) has been obtained with the same machine configuration and general parameters as if a full quadrant were being machined.

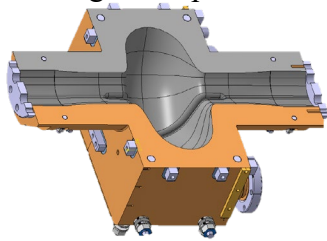


Fig. 1 - SRF Cavity SWELL, two quadrants

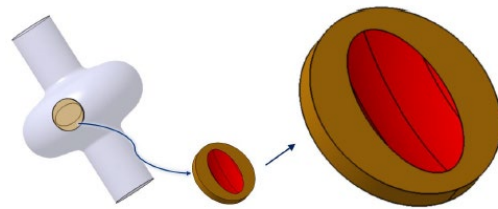


Fig. 2 inner shape of cavity & disc sample geometry

Specific machining parameters -such as cutting conditions, cutting edge radius and friction coefficient- influence the thermomechanical load during milling; they can thus impact surface integrity [6]. In order to benchmark such parameters, nine different scenarios (i.e. sample batches) were produced, permutating cutting tool material and geometry, cutting conditions and machining paths. The milling centre used for the machining of samples was a HERMLE C400. External cooling was used during milling (7% cutting emulsion, mineral miscible oil B-cool MC 610 + tap water). The clamping used was vise Lang Makro grip. All scenarios foresaw the same roughing process, while permutation of parameters was performed during the finishing stages. Since finishing and superfinishing operations have a particular impact on surface integrity as well as geometry of machined parts [7, 8], two sets of reference cutting conditions were used :

- For carbide cutters : $V_c = 245 \text{ m}\cdot\text{min}^{-1}$, $A_p = 0,05 \text{ mm}$, $F_z = 0,03 \text{ mm}\cdot\text{rev}^{-1}\cdot\text{z}^{-1}$, $A_e = 0,091 \text{ mm}$, lateral inclination angle (Tilt) 20°
- For diamond cutters : $V_c = 650 \text{ m}\cdot\text{min}^{-1}$, $A_p = 0,05 \text{ mm}$, $F_z = 0,03 \text{ mm}\cdot\text{rev}^{-1}\cdot\text{z}^{-1}$, $A_e = 0,091 \text{ mm}$, lateral inclination angle (Tilt) 20°

Most tests were carried out with the mentioned reference cutting conditions. On the other hand, cutting speed (V_c) and feed per tooth per revolution (F_z) have a preponderant influence on the surface, compared to the depth of cut (A_p) or radial engagement (A_e) [9], therefore, so-called *aggressive* and *soft* cutting conditions (F_z and V_c increased or decreased by 20% respectively) were also studied for carbide tools.

As mentioned, several different cutting tools were also compared:

- Carbide 1 – Ball end mill ø12 Z4 DLC sp² coated solid carbide (current CERN standard)- as a benchmark cutter to produce control sample,
- Carbide 2 - Ball end mill ø12 Z4 TiAlN-coated solid carbide,
- Carbide 3 - Ball end mill ø12 Z2 uncoated carbide tip - This cutter was chosen for its low edge radius, hence better sharpness due to the absence of coating,
- Diamond - Ball end mill ø12 Z1 monocrystalline diamond.

The impact of tool wear was also considered: the induced degradation of the cut, thus the augmented local plastic deformation are even more pronounced in copper. To simulate this

phenomenon, a tailor-made tool has been ground (“carbide 1” end mill) so as to replicate a typical flank wear (VB) of approx. 0.15mm as one can be seen after a long period of machining. Finally, two milling paths were also studied : unidirectional (so called “parallel planes” which is the standard strategy used for this types of applications) and an outward spiral toolpath.

Table 1 - scenario permutations and corresponding sample nomenclature.

Sample	Strategy	spring pass	Tool	cutting conditions
CONTROL	Unidirectional	No	carbide 1	carbide reference
2	Unidirectional	No	carbide 1	carbide reference +20%
SLOW	Unidirectional	No	carbide 1	carbide reference -20%
4	Unidirectional	No	carbide 2	carbide reference
5	Unidirectional	No	carbide 3	carbide reference
DIA	Unidirectional	No	Diamond	diamond reference
WORN	Unidirectional	No	carbide 1 worn	carbide reference
SPRING PASS	Unidirectional	yes	carbide 1	carbide reference
SPIRAL	Spiral	No	carbide 1	carbide reference

As first qualification ,right after milling operations, the **shape accuracy** of the samples has been measured, thanks to a ZEISS Prismo Ultra 12-24-10 CMM. The shape accuracy was considered in “Best-Fit” configuration.

Surface roughness has also been measured, using a MITUTOYO SV C3100 profilometer, equipped with a 12AAC736 probe (2 μ m radius of acuity). The Average Roughness (Ra), maximum profile height (Rz) and reduced peak height (Rpk) parameters were measured. Rpk provides an indication of the presence of peaks on the surface, particularly useful for studying the effect of a spring pass during milling. Each of them was measured parallel to the feed direction on 3 different lines (parallel to each other), then perpendicular to the feed direction on 3 lines (also parallel to each other). Then, the average was calculated for each direction.

In order for the study to be as consistent as possible with standard SRF manufacturing, following milling operations the samples underwent the surface treatment processes typical for this type of SRF cavities.

Prior to coating, SRF cavities undergo an **Electro-polishing (EP)** process, which firstly aims at reducing the surface roughness left from previous manufacturing operations. This surface roughness is detrimental to cavity performance and can cause electrical breakdown during service. The bath used for SWELL cavities is composed of 45% (vol.) Butanol (C₄H₁₀O) and 55% phosphoric acid (H₃PO₄). The Material removal rate is approximately 1 μ m/min. The thickness removed is around 12 μ m on the basis of the best results to the present day. The SWELL samples in this study are treated with the same EP procedure as described above for a full cavity. The samples are then immersed in sulfamic acid for 1 minute to remove surface oxides and then into ammonium citrate for 5 minutes to passivate the surface and prevent further oxide growth.

The samples have then been Nb-coated via **High-Power Impulse Magnetron Sputtering (HiPIMS)** system. HiPIMS generates high peak-currents, leading to increased ionization of the sputtered material compared to conventional methods like Direct Current Magnetron Sputtering (DCMS). This allows for precise control of the ion bombardment energy by applying a negative voltage at the substrate (DC substrate bias). This enables much higher impinging energies, which in turn result in denser films with improved RF performance [10]. The main parameters used for the coating of the SWELL cavity samples can be seen in Table 2:

Table 2 – main parameters of HiPIMS coating process

average power	1.2 [kW]
substrate temperature during deposition	150 [°C]
Krypton pressure	2.3/2.4x10 ⁻³ [mbar]
substrate-to-ground voltage	- 75 [V] (DC)
HiPIMS pulse length	200 [µS]
HiPIMS signal frequency	100 [Hz]
Deposition time	6 [h]

These parameters enable discharge voltages of 625 V and ion peak currents of around 159 A, resulting in a niobium layer of around 6 µm. Further details about the sputtering system and deposition procedure can be found in [11].

Presence of dislocations on the subsurface and coated layers has been evaluated, as **dislocation density** is believed to be one of the driving parameters affecting poor SRF performance of the Niobium coating. Dislocations in the top layer were evaluated by using the **GI-XRD** configuration in a BRUKER D8 DISCOVER X-ray diffractometer, equipped with Eiger 2R 500K detector. The incident Theta angle was fixed in two degrees. This shallow angle ensures that the X-rays interact exclusively with the material's surface enhancing the diffracted signal from the copper after machining or EP and subsequently from the Nb coating. In the present study, the collected signal came from a depth of approximately two microns for copper specimens, and approximately half micron for the Nb coated ones. Based on best practices, the surface scan in 2 thetas was chosen (with the receiver position fixed at 2°), a step size of 0.07° with an exposure time of 1.5 seconds per step and a 0.2 mm slit.

The obtained x-ray diffractograms were then processed using the MAUD software [12]. Full Rietveld refinement is performed to extract the crystallites' size, *D*, the microstrain ϵ , and the lattice parameter, *a*. Instrumental widening is corrected using a corundum sample. The dislocation density was calculated as

$$\rho_D = 2\sqrt{3} \frac{\langle \epsilon^2 \rangle^{1/2}}{D \times b} \quad (1)$$

where ρ_D is the dislocation density (m⁻²), *D* is the crystallite size (m), and *b* is the burger vector expressed as $\frac{a\sqrt{3}}{2}$ (m) for BCC materials such as Nb and $a\sqrt{2}$ for FCC materials such as Cu.

The thickness of the Cu **substrate layers affected by milling** was estimated by **Focused Ion Beam Scanning Electron Microscopy** (FIB - SEM). The instrument used for FIB-SEM was a ZEISS XB 540, equipped with InLens Secondary Electron detector (InLens) and STEM (Scanning Transmission Electron Microscope) detector. The set-up used for FIB-SEM analysis mainly involves an FIB gun, a platinum sprayer used to protect the extreme surface of the FIB dispersion, and an electron detector for producing usable images. The FIB cut was initially made parallel to the milling marks, so as to observe any sub-surface grain elongation effects.

Results and Discussion

Shape Accuracy

Fig. 3 shows the typical shape accuracy measurements for one of the samples, while - values of shape deviation for each scenario produced. Fig. 4 summarizes the highest absolute values of shape deviation, measured for each sample. It can be noted how the samples machined by lower cutting conditions (SLOW) and by using a spiral path (SPIRAL) are particularly unfavourable for obtaining an accurate geometry, showing 0,031 mm and 0,038 mm of shape deviation respectively. For the SLOW sample, the reason may be found in the less efficient cutting process and more pronounced ploughing effect. In the case of SPIRAL sample, these deviations can be linked to the high acceleration of the machine-tool axes movements. Moreover, since there are several axes moving simultaneously with a frequent change of direction of movement. Therefore, there is an accumulation of interpolation errors and pivot point error resulting in lowered accuracy [13]. Near-to-best shape accuracy can be found in DIA sample. This can be attributed to several factors, among which cutting edge sharpness and low copper/diamond chemical affinity.

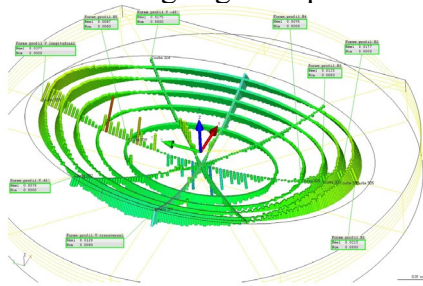


Fig. 3 - shape deviation visualised in space, according to the best-fit criterion. sample "SPIRAL"

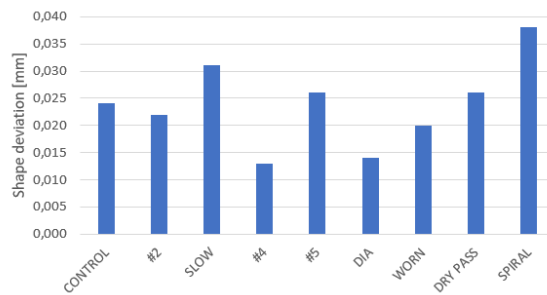


Fig. 4 - values of shape deviation for each scenario produced.

Surface Roughness

Fig. 5 shows the results for each sample, in terms Ra, Rz, Rpk, which represent some of the most important roughness parameters for SRF. The Ra target is 1.6 μm . The other parameters are not currently defined in the technical specification for SWELL cavities.

It must be noted that the highest values are obtained when measuring roughness in the circumferential direction and are therefore the ones shown in figure.

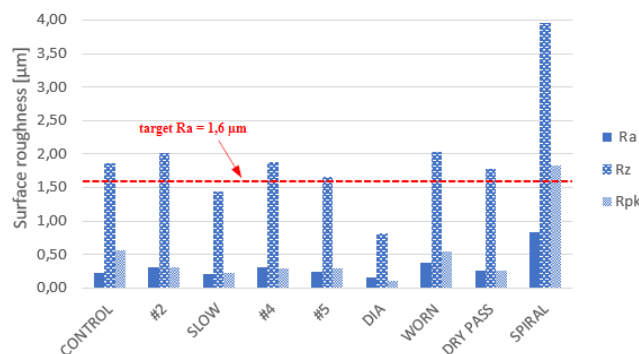


Fig. 5 - overview of surface roughness criteria

The measured values show that all scenarios have Ra values below the maximum target value. The roughness values obtained with a diamond cutter (DIA) are the lowest in the study (Ra 0,16 μm , Rz 0,82 μm , Rpk 0,11 μm) followed by those of the sample milled with SLOW conditions. The low roughness obtained by the diamond cutter can be attributed to several factors. As shown

in [14], diamond has a low chemical affinity ("lattice mismatch") with copper, which translates on a macroscopic scale into a lower friction coefficient than other material pairs (e.g. carbide/copper or TiAlN/copper). This coefficient reduces copper's grip on diamond, thereby reducing the ploughing effects mentioned above. The reduction of cutting conditions (SLOW) also results in a relatively smooth surface compared to the control sample (CONTROL).

On the contrary, the sample milled by spiral trajectory (sample SPIRAL) seems to give high values of surface roughness (Ra 0,83 μm , Rz 3.96 μm , Rpk 1.84 μm). This can be partly explained by the fact that several of the machine's linear axes are in motion during this trajectory, reducing the system's rigidity on the one hand, and accumulating the backlash of several axes on the other. Another reason is the direction of measurement since in this scenario the roughness probe's path goes through multiple valleys and peaks which should theoretically be bigger than in the cutter's feed direction.

As expected, the sample milled with the worn cutter (WORN) also gives higher values. The sample milled with a spring pass (SPRING PASS) shows values of Ra and Rz that are almost identical with the control sample; the value of Rpk is though 50% smaller than with the control sample. This can be explained by the presence of micro-peaks which can be as a result of ploughing phenomenon occurring during machining and therefore imperfect shearing of the material. The following spring pass eliminates those pics without touching the core of the material. In any case, the amelioration seen with the additional spring pass is of high interest and will be implemented in the next productions requiring high quality of surface finish.

Dislocation Density Comparison

The sample DIA is showing overall low degree of affectation in both machined and coated samples, proving to be the best amongst all samples in terms of low deformation of the subsurface. The small radius of its cutting edge seems to result in minimal material affectation. In addition to its sharp cutting edge and low chemical affinity with copper, such good results can be traced on the excellent thermal conductivity of single-crystal diamond : 5 times higher than copper [15], whereas the thermal conductivity of carbide is 4 times lower than that of copper, and therefore 20 times lower than that of diamond.

Oppositely, sample SLOW carries the highest estimated dislocation density in OFE copper substrate and one of the highest in niobium coating. This phenomenon is attributed to the ploughing effects which occurs more in these conditions. The dislocation density in the niobium layers of samples WORN and SPIRAL record highest among all samples. For what concerns WORN, this may be more easily attributed to more pressure being applied on the surface due to larger contact area tool/clearance face (worn). Hence mechanical compressive stress increases. For what concerns SPIRAL, reason may be due to the machine tool's lower rigidity and accumulated backlash, due to frequent axis inversion during machining. This may have disturbed the finishing pass having an impact on dislocation density.

As demonstrated on Fig. 7, there is an impact of the existing density of dislocation of the copper substrate to the dislocation density of the deposited niobium. One should remind that the EP process remove a significant amount of the copper surface. Even though a weak direct correlation, a basic trend could be estimated. Dislocation density is quite sensitive to sample preparation and existing lattice structure. A way to increase the robustness of the correlation could be through an extensive campaign of measurement to average its inherent variability. On the other hand, the effects of substrate dislocation and similar 'defects' may not be so easy to notice, and the optimisation of substrate thus still plays a role. It can be seen how dislocation densities in electropolished Cu strongly do not correlate with those of either Cu substrate after machining or Nb after coating; Their values are also greatly smaller than those in machined Cu and in the final Nb layer. Some sort of dislocation memory – or defects not observable or yet deemed of

interest- must thus be present and are still greatly influence the end result of coating. Due to this, the control and minimisation of sublayer defects induced during milling is still paramount.

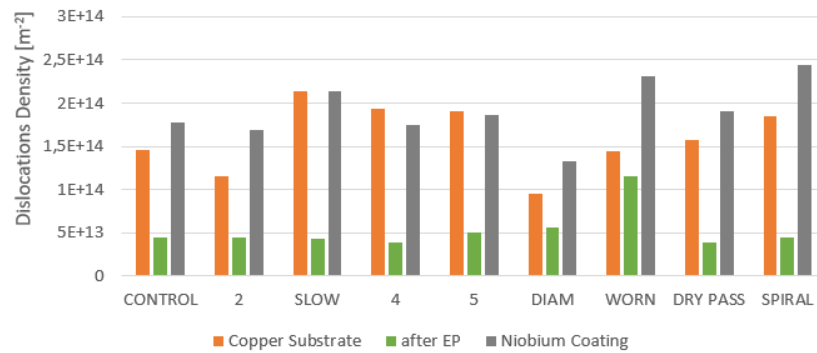


Fig. 6 - estimated dislocation density

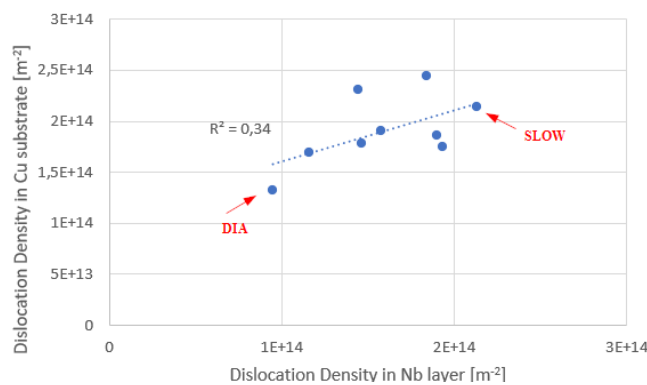


Fig. 7 -The dislocation density in the copper substrate vs. the dislocation density in Nb layer.

Estimation of the Affected Layer

Based on previous GI-XRD results, the FIB-SEM cross sectional inspection of the samples DIA (lowest dislocation density) and SLOW (highest dislocation density) are further developed in this paper (Fig. 8 and Fig. 9 respectively), as these showed extreme dislocation density values in the Cu substrate after machining (sample DIA with the lowest dislocation density and SLOW with the highest).

An affected band is discernible on the near surface of the copper material in the DIA sample, machined with a diamond tool (Fig. 10). The estimated thickness remains consistent for both the cross-sectional view (aligned with the machining marks) and the view perpendicular to them. However, in the latter case, there is a slight increase in variation along the cut. In contrast to the diamond-milled sample, machining marks are clearly visible on SLOW sample (Fig. 11).

An affected band - more prominently evident on the SLOW sample than on the DIA sample, and with an aspect similar to the one discussed in reference [16]- indicates a greater degree of plastic deformation and, consequently, a more substantial density of dislocations. This hypothesis aligns consistently with the results obtained from the GIXRD analyses.

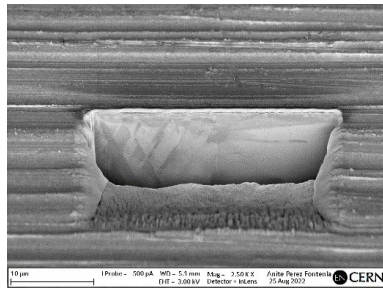


Fig. 8 – Sample DIA: general FIB-SEM overview (InLens, mag. x2'500)

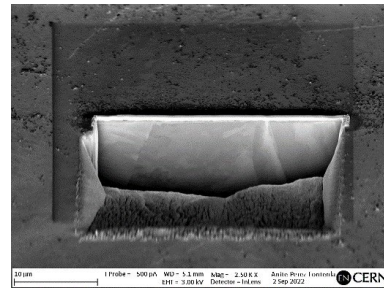


Fig. 9 - Sample SLOW: general FIB-SEM overview (InLens, mag. x2'500)

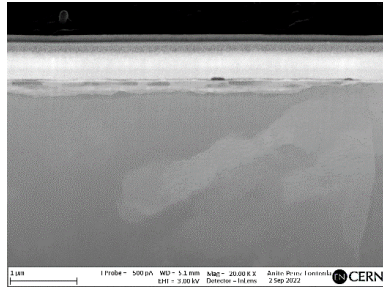


Fig. 10 – Sample DIA: FIB-SEM cross-section (InLens, mag. x20'000)

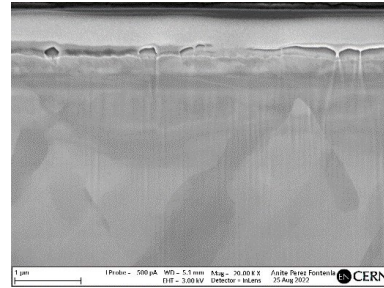


Fig. 11- Sample SLOW: FIB-SEM cross-section (InLens, mag. x20'000)

Fig. 12 provides the result of affected layer thickness for all samples in the study. In order to account for the embedded variability of the process and of the measurement, a minimum of three measurements were conducted per sample, to derive the representative mean value and standard deviation (the latter in parenthesis in the abscissa label).

Specifically for the DIA sample, measurements yield results ranging from 162 to 408 nm; while the SLOW sample displays affected thickness varying from 508 to 1597 nm. It can though be noted how the SLOW sample is not the one embedding worst values of affected layer thickness.

This result is in line with the results of GI-XRD: the presence of defects follows a trend where the best (DIA) and worst cutting conditions produce loosely consistent effects. Nevertheless, the worst performing cutting condition for the copper substrate (SLOW) are not the ultimately worst for the Nb layer (WORN).

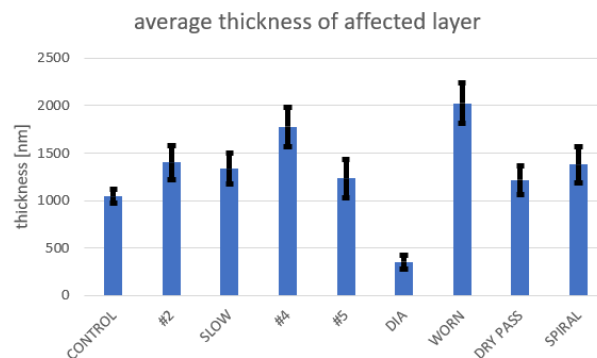


Fig. 12 - average thickness of affected layer. The standard deviations are visualized for each sample.

Conclusion and Next Steps

The study has allowed to further the insights on the impact of machining on the quality of the subsurface copper layer and thus on the superconducting niobium layer of SRF machined cavities. The influence of edge radius on changes in surface integrity emerges as a significant factor. Even low values of tool wear stand out as the parameter greatly affecting dislocation density of the copper substrate. Though its effects on measured final dislocation of the SRF layer seem to be reduced, optimal conditions for Nb coating are difficult to obtain, especially on complex geometries far from the samples studied; wear should be kept under close control, and it appears clearly that 0.15mm flank wear is already above acceptable limit.

The use of diamond tool stands out as the best configuration for minimising dislocation density of both copper substrate and Nb layer. Additional studies will be performed in the space of cutting parameters with this tool, in order to find an optimal setup.

In addition, results of dislocation density and affected layer open the door to novel considerations with respect to current state of the art: substrate defects such as dislocation density may be only one of the driving factors for optimal Nb layer performance. This is why RF performance checks, EBSD as well as complementary GIXRD analyses, are in progress at the time of writing. Such results will be needed to finalise the link between substrate and SRF layer quality with respect to final radiofrequency performance; though such link has been obtained for surfaces yielding from different processes (shaping, turning), milling tests results are in any case needed to validate the above considerations on dislocation density.

Further tests -with identical milling cutters differing only in edge radius- will be conducted to provide additional insight; additionally, a more comprehensive description of cutter geometry at the cutting zone level, encompassing factors like surface "reflection" and clearance angles, would enhance our understanding of the mechanisms at play during milling. It might be conclusive to investigate the type and rate of tool wear. Only flank wear has been taken into account but due to the harsh behaviour of OFE copper, built-up edge of crater wear could be seen and would greatly modify the tool/copper interface phenomenon.

Acknowledgements

The authors would like to acknowledge the following CERN colleagues, for their instrumental support in preparation of the samples and of the tests: Romain Ninet, Alan Saillet, Philippe Richerot, Dominique Pugnât, Maciej Burkowski, Ahmed Cherif, Louise Viezzi, Marc Thiebert and Serge Forel.

References

- [1] C. P. A. Carlos et al., Nb/Cu thin film HiPIMS coatings optimization for SRF applications, FCC Week 2022, Paris, France, 30 May - 03 June 2022.
- [2] A. Camelin et al. Experimental analysis of subsurface integrity during fine turning of OFE copper for radiofrequency cavity manufacturing. *Journal of Materials Processing Technology*. 302. (2021) 117483. <https://doi.org/10.1016/j.jmatprotec.2021.117483>
- [3] A. Plaçais et al., Multipactor studies for the FCC-ee superconducting SWELL cavities, (2023).
- [4] M. Benedikt et al., Future Circular Collider - European Strategy Update Documents, (2019).
- [5] I. Perez et al., Effect of cutting speed on the surface integrity of face milled 7050-T7451 aluminium workpieces. *Procedia CIRP*. 71 (2018) 460-465. <https://doi.org/10.1016/j.procir.2018.05.034>
- [6] K. Gutzeit et al., Influence of the cutting-edge radius on tool wear during cryogenic machining with cemented carbide end mills. (2022).

- [7] L. Denguir, José Outeiro, Guillaume Fromentin, Vincent Vignal, Rémy Besnard: Influence of cutting process mechanics on surface integrity and electrochemical behavior of OFHC copper. *Procedia CIRP* 13 (2014) 186 – 191. <https://doi.org/10.1016/j.procir.2014.04.032>
- [8] J. P. Davim et al: *Machining*, edition Springer, Department of Mechanical Engineering, University of Aveiro, Aveiro, Portugal. (2008).
- [9] Y. Zenchao, X. Yang, L. Yan, X. Jin, W. Quandai: The effect of milling parameters on surface integrity in high-speed milling of ultrahigh strength steel. *Procedia CIRP* 71 (2018) 83–88. <https://doi.org/10.1016/j.procir.2018.05.076>
- [10] M. Arzeo et al., Enhanced radio-frequency performance of niobium films on copper substrates deposited by high power impulse magnetron sputtering. *Supercond. Sci. Technol.* 35 (2022) 054008. <https://doi.org/10.1088/1361-6668/ac5646>
- [11] G. Rosaz et al., Niobium thin film thickness profile tailoring on complex shape substrates using unbalanced biased High Power Impulse Magnetron Sputtering, *Surf. Coat. Technol.* 436 (2022) 128306. <https://doi.org/10.1016/j.surfcoat.2022.128306>
- [12] L. Lutterotti et al., A friendly java program for material analysis using diffraction. (1999).
- [13] A. SAILLET et al., Evaluation of computer-aided manufacturing software accuracy for high precision machining, *euspen's 20th International Conference & Exhibition*, Geneva, CH, June 2020.
- [14] J. Ma, University of Waikato, New Zealand: Investigation on the interface structure and thermal conductivity of hot-forged Cu/ (Ti/W-coated)-diamond composites. (2020).
- [15] J. E. Graebner : Thermal Conductivity of Diamond. In : Pan, L.S., Kania, D.R. (eds) *Diamond : Electronic Properties and Applications*, (1995)285-318, editor : Springer. https://doi.org/10.1007/978-1-4615-2257-7_7
- [16] S. Breumier et al., High strain rate micro-compression for crystal plasticity constitutive law parameters identification. (2021). <https://doi.org/10.1016/j.matdes.2020.108789>